Essential role for a long-term depression mechanism in ocular dominance plasticity

Essential role for a long-term depression mechanism in ocular dominance plasticity

Bong-June Yoon[a,b,1], Gordon B. Smith[a,1], Arnold J. Heynen[a,1], Rachael L. Neve[c], and Mark F. Bear[a,2]

[a]Howard Hughes Medical Institute, The Picower Institute for Learning and Memory, [c]Department of Brain and Cognitive Sciences, Massachusetts Institute of Technology, Cambridge, MA 02139; and [b]College of Life Sciences and Biotechnology, Korea University, Anam-dong, Seongbuk-Gu, Seoul 136–701, Korea

Edited by Richard L. Huganir, Johns Hopkins University School of Medicine, Baltimore, MD, and approved April 14, 2009 (received for review February 5, 2009)

The classic example of experience-dependent cortical plasticity is the ocular dominance (OD) shift in visual cortex after monocular deprivation (MD). The experimental model of homosynaptic long-term depression (LTD) was originally introduced to study the mechanisms that could account for deprivation-induced loss of visual responsiveness. One established LTD mechanism is a loss of sensitivity to the neurotransmitter glutamate caused by internalization of postsynaptic α-amino-3-hydroxy-5-methyl-4-isoxazole propionic acid receptors (AMPARs). Although it has been shown that MD similarly causes a loss of AMPARs from visual cortical synapses, the contribution of this change to the OD shift has not been established. Using an herpes simplex virus (HSV) vector, we expressed in visual cortical neurons a peptide (G2CT) designed to block AMPAR internalization by hindering the association of the C-terminal tail of the AMPAR GluR2 subunit with the AP2 clathrin adaptor complex. We found that G2CT expression interferes with NMDA receptor (NMDAR)-dependent AMPAR endocytosis and LTD, without affecting baseline synaptic transmission. When expressed in vivo, G2CT completely blocked the OD shift and depression of deprived-eye responses after MD without affecting baseline visual responsiveness or experience-dependent response potentiation in layer 4 of visual cortex. These data suggest that AMPAR internalization is essential for the loss of synaptic strength caused by sensory deprivation in visual cortex.

amblyopia | glutamate receptor trafficking | monocular deprivation | visual cortex

The earliest and most dramatic effect of monocular deprivation (MD) is the severe loss of visual cortical responsiveness to the deprived eye (deprivation amblyopia). Over the past 20 years, the hypothesis has been advanced that untimely or weak activation of cortical neurons by deprived-eye inputs is a trigger for synaptic depression in visual cortex (1, 2). This idea received strong support with the discovery of homosynaptic long-term depression (LTD), a persistent modification of transmission at synapses activated by various types of electrical stimulation. LTD has been studied intensively to uncover the mechanisms that make synapses weaker (3). In sensory cortex, most forms of LTD require activation of NMDA receptors (NMDARs) (4–7) and, indeed, blockade (8, 9) or genetic deletion of NMDARs (10) prevents the ocular dominance (OD) shift after MD. However, NMDAR blockade affects multiple forms of plasticity. Thus, it has been difficult to test the specific hypothesis that LTD mechanisms per se contribute to the OD shift, a problem compounded by the fact that it is now clear that there are multiple mechanisms that could compensate for one another (4, 11).

The most advanced understanding of a mechanism for NMDAR-dependent LTD comes from studies of hippocampus. Here, it has been shown that weak or sustained activation of NMDARs triggers the endocytosis of postsynaptic α-amino-3-hydroxy-5-methyl-4-isoxazole propionic acid receptors (AMPARs) (12) via a specific interaction of the GluR2 C-terminal tail with the AP2 clathrin adaptor complex (13). This interaction can be selectively disrupted with a peptide (KRMKLNINPS), we term G2CT, that mimics the GluR2 amino acid sequence required for the AP2 interaction. Lee et al. (13) showed that G2CT has remarkable selectivity when introduced postsynaptically, blocking NMDAR-stimulated AMPAR endocytosis and hippocampal LTD without affecting baseline transmission or AMPA-stimulated AMPAR internalization.

Recent work has shown that there are significant laminar differences in the mechanisms of both LTD and OD plasticity in mouse visual cortex (4, 14). However, LTD of the radial input to layer 4 closely resembles that in hippocampal area CA1, notably including sensitivity to intracellularly loaded G2CT. Therefore, we reasoned that if it could be introduced intracellularly in vivo, the G2CT peptide could be used to assess the contributions of both NMDAR-dependent AMPAR internalization and LTD in layer 4 to visual cortical plasticity.

Here, we show that it is possible to deliver G2CT peptide to neurons by using an HSV vector. We find that virally expressed G2CT blocks NMDA-stimulated AMPAR endocytosis in cortical neurons and synaptically induced LTD in layer 4 of visual cortex. Expression of G2CT in layer 4 neurons in vivo is sufficient to completely prevent depression of deprived-eye responses after brief MD, while leaving intact the mechanisms of experience-dependent synaptic enhancement. We conclude that AMPAR endocytosis plays a critical role in the loss of visual responsiveness after MD.

Results

Viral Expression of G2CT Blocks NMDA-Stimulated AMPAR Internalization in Cultured Visual Cortical Neurons. We used an HSV vector (15, 16) to deliver green fluorescent protein (GFP) and G2CT under separate promoters (HSV-G2CT) (Fig. S1*A*). A virus expressing GFP alone was used as a control (HSV-GFP). To confirm that the G2CT peptide could be expressed in infected neurons at a level sufficient to block NMDAR-dependent AMPAR endocytosis, we incubated cultured occipital cortical neurons with HSV vectors and, 24 h later, examined the effect of brief NMDA treatment (20 μM, 5 min) on surface-expressed AMPARs. We found that ≈90% of the cultured neurons expressed GFP at 24 h postinfection (Fig. S1*B*) and that HSV-G2CT infected neurons exhibited normal morphological characteristics (Fig. S1*C*). In accordance with previous reports, we found that NMDA treatment significantly reduced the number of AMPARs present on the plasma membrane in uninfected

Author contributions: B.-J.Y., G.B.S., A.J.H., and M.F.B. designed research; B.-J.Y., G.B.S., and A.J.H. performed research; R.L.N. contributed new reagents/analytic tools; B.-J.Y., G.B.S., A.J.H., and M.F.B. analyzed data; and B.-J.Y., G.B.S., A.J.H., and M.F.B. wrote the paper.

The authors declare no conflict of interest.

This article is a PNAS Direct Submission.

Freely available online through the PNAS open access option.

[1]B.-J.Y., G.B.S., and A.J.H. contributed equally to this work.

[2]To whom correspondence should be addressed. E-mail: mbear@mit.edu.

This article contains supporting information online at www.pnas.org/cgi/content/full/0901305106/DCSupplemental.

control cultures as well as in cultures infected with HSV-GFP. However, HSV-G2CT infection completely blocked the NMDA-stimulated loss of surface AMPARs (Fig. 1 *A* and *B*). Quantification of the level of surface expressed AMPARs under baseline (non-NMDA treated) conditions showed no significant difference between noninfected, HSV-GFP-, and HSV-G2CT-infected cultures (100 ± 6.5%, 137.7 ± 21.4%, 120.1 ± 16.1%, respectively), suggesting that expression of the G2CT peptide does not affect basal AMPAR trafficking and surface expression. The ability of G2CT to interfere with the stimulated endocytosis of GluR1 is likely due to an effect on heteromeric GluR1/GluR2 receptors.

To confirm that the observed inhibition of AMPAR endocytosis by the G2CT peptide was not due to a general disruption of clathrin-mediated endocytosis, but rather the result of a specific disruption in the association between AP2 and AMPARs, we examined the clathrin-dependent endocytosis of transferrin receptors (TfRs). After transferrin application, levels of internalized TfRs were comparable in noninfected, HSV-GFP-, and HSV-G2CT-infected cultures (Fig. 1*C*).

Viral Expression of G2CT Blocks NMDA-Stimulated AMPAR Internalization in Visual Cortical Slices. We next examined the in vivo efficiency of HSV-mediated infection in mouse visual cortex and tested the ability of HSV-G2CT to block NMDAR-dependent AMPAR endocytosis in acutely prepared slices. Robust and sustained GFP expression was observed after infections targeted to layer 4 of visual cortex (Fig. 1*D*). GFP expression was detected as early as 1 day post infection, and expression was maintained at high levels through at least 6 days post infection. To determine which cell types were infected, we conducted a series of experiments in which GFP+ cells were immunocytochemically double-labeled with a neuronal marker (Neu-N) or a marker of inhibitory interneurons (γ-amino butyric acid, GABA). Eighty-nine percent of GFP+ cells ($n = 446$) were positive for NeuN, confirming previous observations that HSV is highly neurotropic (16). Interestingly, even though the infected volume contained many GABA+ cells ($n = 165$), very few of these also contained GFP ($n = 3$ of 165; 1.8%) (Fig. 1*E*). This unexpected difference in infectivity suggests that the effects of G2CT expression are primarily because of disruptions in AMPAR endocytosis in excitatory neurons.

To assess whether G2CT expression after in vivo infection was sufficiently strong to interfere with activity-dependent AMPAR endocytosis, slices prepared 48 h postinfection were treated with NMDA (100 μm, 15 min; Fig. 1*F*). In noninfected visual cortex, NMDA produced a significant reduction of surface-expressed AMPARs (GluR1: 77.3 ± 6.6% of control, $n = 5$, $P < 0.05$; GluR2/3: 84.7 ± 3.5% of control, $n = 5$, $P < 0.05$; Fig. 1*G*), whereas internalization was blocked in HSV-G2CT infected cortex (GluR1: 91.0 ± 9.4% of control, $n = 5$, $P > 0.40$; GluR2/3: 105 ± 12.4% of control, $n = 5$, $P > 0.69$).

Pairing-Induced LTD in Visual Cortical Layer 4 Spiny Neurons Is Blocked by Viral Expression of G2CT. We next determined whether viral expression of G2CT was sufficient to interfere with LTD of excitatory postsynaptic currents (EPSCs) evoked in layer 4 neurons by white matter stimulation, a process known to be sensitive to the G2CT peptide (4). HSV-G2CT was injected into 1 hemisphere of visual cortex, and slices were prepared 48–72 h post infection from both hemispheres, with the uninfected cortex serving as a control (Fig. 2*A*). Pairing 1 Hz presynaptic stimulation with modest postsynaptic depolarization reliably elicited LTD in uninfected neurons (71.8 ± 2.2% of baseline, $n = 5$ cells from 5 mice, $P < 0.05$, paired t test), consistent with previous findings (4). However, LTD was absent in G2CT-expressing cells (96.7 ± 10.1% of baseline, $n = 5$ cells from 5 mice, $P > 0.2$, paired t test; Fig. 2*B*). We therefore conclude that infection of

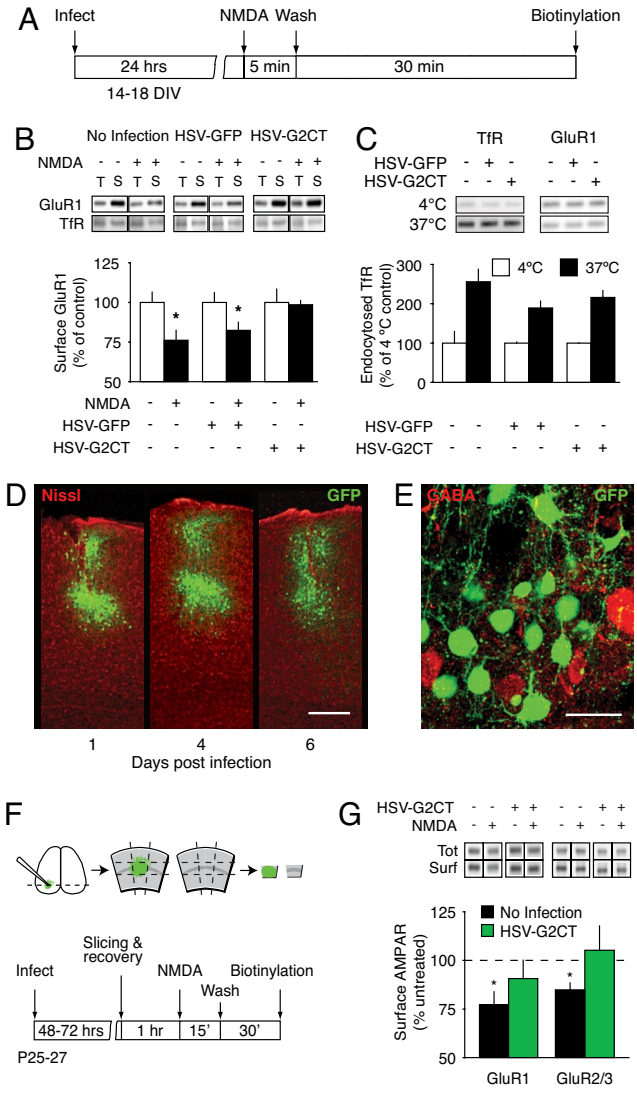

Fig. 1. Viral expression of G2CT blocks NMDA-stimulated AMPAR internalization in visual cortical cultures and slices. (*A*) Experimental design for cortical culture experiments. (*B*) HSV-G2CT infection prevents NMDA-stimulated AMPAR internalization. NMDA treatment produced a significant reduction of surface-expressed GluR1 in noninfected cultures (mean ± SEM of untreated control: 76.2 ± 6.1%, $n = 8$, $P < 0.05$) and HSV-GFP infected cultures (82.4 ± 5.0%, $n = 8$, $P < 0.05$), but not in HSV-G2CT-infected cultures (98.6 ± 2.6%, $n = 8$, $P > 0.5$). Note that surface GluR1 levels under control conditions (no infection, $n = 8$; HSV-GFP, $n = 12$; HSV-G2CT, $n = 6$) were comparable between all groups, indicating that the G2CT peptide does not affect basal AMPAR trafficking (T, total; S, surface). (*C*) Viral expression of G2CT does not affect transferrin receptor (TfR) endocytosis. To rule out a nonspecific effect on clathrin-mediated endocytosis, the level of surfaced expressed TfR was measured after transferrin application. Levels of internalized TfR at 37 °C were comparable across cultures, and nonspecific GluR1 internalization was not observed. (*D*) GFP expression in neurons after injection of HSV-G2CT into layer 4 of visual cortex is robust and sustained (Scale bars, 200 μm.) (*E*) No colocalization of GFP+ (green cells) and GABA+ (red cells, marked with asterisks) indicates HSV infection is restricted primarily to excitatory neurons (Scale bar, 25 μm.) (*F*) Experimental design for slice preparation experiments. Visual cortical slices were obtained 48–72 h after in vivo infection, and a region in the middle of the cortical thickness, corresponding to layer 4, was microdissected from both the HSV-infected and contralateral (noninfected) visual cortices. After recovery, slices were treated with NMDA (100 μM, 15 min), and 30 min later, surface proteins were biotinylated and immunoblot analysis performed. (*G*) NMDA treatment produced a significant reduction of surface-expressed AMPARs in noninfected visual cortex (GluR1: 77.3 ± 6.6% of control, $n = 5$, $P < 0.05$; GluR2/3: 84.7 ± 3.5% of control, $n = 5$, $P < 0.05$), whereas internalization was blocked in HSV-G2CT infected cortex (GluR1: 91.0 ± 9.4% of control, $n = 5$, $P > 0.40$; GluR2/3: 105 ± 12.4% of control, $n = 5$, $P > 0.69$).

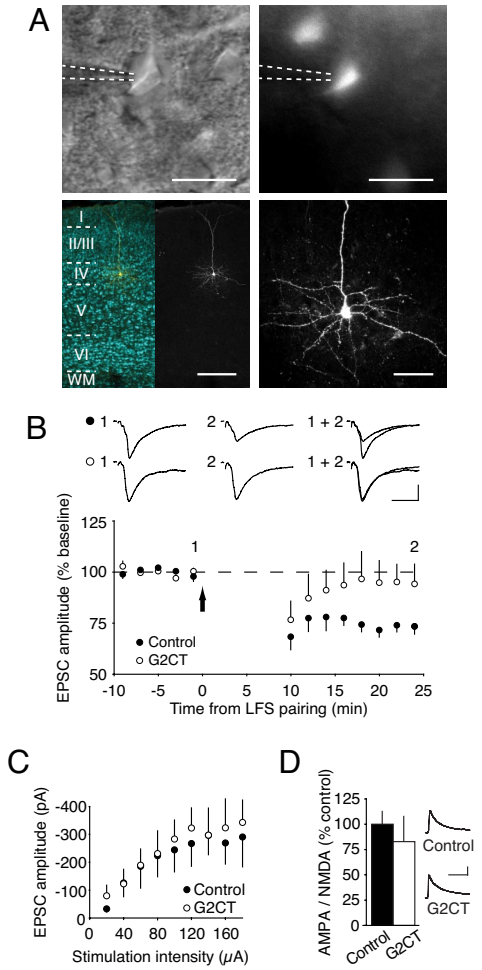

Fig. 2. Expression of G2CT blocks pairing-induced LTD in layer 4 of visual cortex. (*A*) Recordings were made from infected GFP positive cells in layer 4 of visual cortex. (*Top*) IR-DIC (*Left*) and GFP (*Right*) images showing target cell before seal formation with recording pipet outlined in white. (*Bottom Left*) Nissl stained section indicating laminar borders. A biocytin filled and stained neuron is shown overlying the Nissl stain in yellow, and alone to the right. (*Bottom Right*) Higher magnification image of cell shown in bottom left. Note prominent apical dendrite and descending basal dendrites, features indicative of a layer 4 star pyramidal neuron (Scale bars, 25, 25, 200, 50 μM for top left to bottom right, respectively.) (*B*) Pairing-induced LTD is blocked in neurons infected with HSV-G2CT. Traces are representative EPSCs averaged over 6 consecutive responses recorded at times shown in summary graph below (Scale bars, 10 ms, 100 pA.) Lower graph shows the time course of average EPSC amplitude in control and G2CT-expressing cells. A 1 Hz pairing protocol was delivered at time indicated by arrow. LFS pairing resulted in significant LTD in control (71.8 $\pm$ 2.2% of baseline, $n = 5$, $P < 0.05$, paired t test) but not G2CT expressing (96.7 $\pm$ 10.1% of baseline, $n = 5$, $P > 0.2$, paired t test) cells. A significant between group difference in LTD magnitude is also observed ($P < 0.05$, unpaired t test). (*C*) G2CT expression does not affect basal synaptic transmission from white matter to layer 4 assayed via input-output relationships. (*D*) AMPA/NMDA ratios in G2CT-expressing neurons are comparable to noninfected controls. Traces at right show representative EPSCs recorded at +40 mV (Scale bars, 50 ms, 400 pA.) Histogram presents average AMPA/NMDA ratios, normalized to control. No significant difference was observed between groups (control: 100 $\pm$ 12.5%, $n = 7$; G2CT: 82.8 $\pm$ 24.5%, $n = 6$; $P > 0.5$).

visual cortex in vivo with HSV-G2CT is sufficient to block synaptic depression arising from AMPAR endocytosis.

It is possible that infected neurons fail to exhibit synaptic plasticity because they are injured. However, intrinsic electrophysiological properties, such as membrane potential (V_m), membrane resistance (R_m), and membrane capacitance (C_m), of noninfected control cells ($n = 12$) and HSV-G2CT infected neurons ($n = 8$) were indistinguishable (V_m: -68.3 ± 3.0 vs -68.4 ± 4.9 mV, $P > 0.5$; R_m: 256.3 $\pm$ 30.0 vs 292.0 $\pm$ 31.0 MΩ, $P > 0.4$; C_m: 61.6 $\pm$ 5.2 vs 61.9 $\pm$ 8.7 pF, $P > 0.5$). Similarly, when input-output curves and AMPA/NMDA ratios were examined in control and G2CT-expressing cells, no significant differences were observed (input-output: $n = 5$ control; 4 G2CT; repeated measures ANOVA, $P > 0.5$; Fig. 2*C*; AMPA/NMDA: control: 100 $\pm$ 12.5% of control, $n = 7$; G2CT: 82.8 $\pm$ 24.5% of control, $n = 6$; $P > 0.5$; Fig. 2*D* and Fig. S2). Thus, the impairment of LTD cannot be explained by altered excitability or reduced NMDAR expression in the infected neurons.

G2CT Expression Blocks MD-Induced Synaptic Depression, but Not Experience-Dependent Synaptic Enhancement In Vivo. The above results suggested that it would be feasible to use HSV-mediated delivery of G2CT to test the hypothesis that OD plasticity requires AMPAR internalization. Before performing these experiments, however, we first ensured that HSV-G2CT infection does not alter the baseline amplitude of visually evoked potentials (VEPs) in vivo. We targeted layer 4 of visual cortex with HSV-GFP ($n = 14$) or HSV-G2CT ($n = 17$) injections and implanted an electrode at the same site through which we could monitor VEPs before random assignment of animals to either the "MD" or "SRP" groups (see *Results*). This analysis revealed no significant differences between HSV-GFP or HSV-G2CT infected groups (contralateral eye response, HSV-GFP 174.7 $\pm$ 13.5 μV vs HSV-G2CT 175.1 $\pm$ 10.9 μV, t test: $P > 0.9$; ipsilateral eye response, HSV-GFP 98.7 $\pm$ 8.4 μV vs HSV-G2CT 98.7 $\pm$ 7.7 μV, t test: $P > 0.9$, Fig. 3*C*).

In a subset of infected animals, we monitored VEPs before and after 3 days of MD (Fig. 3 *A* and *B*). Within this subset of mice, there was no significant difference in pre-MD baseline VEP amplitudes between HSV-GFP and HSV-G2CT animals (deprived-eye $P > 0.5$; nondeprived eye $P > 0.8$; unpaired t test). Previous experiments using this chronic VEP method have shown that closing the contralateral eyelid for 3 days is sufficient to saturate deprived-eye response depression without affecting open-eye responses (15, 17). Consistent with these findings, we observed that 3 days of MD in HSV-GFP infected animals resulted in a significant decrease in deprived-eye responses (baseline 184.9 $\pm$ 23.2 vs post-3 d MD 119.3 $\pm$ 15.3 μV, $P < 0.01$, paired t test, $n = 7$), whereas nondeprived-eye responses remained unchanged (baseline 109.6 $\pm$ 10.3 vs post-3 d MD 104.2 $\pm$ 15.1 μV, $P > 0.5$, paired t test; Fig. 3*D*). These findings demonstrate that viral infection per se does not impede normal OD plasticity. However, we found that viral infection with HSV-G2CT completely blocked the deprived eye depression associated with 3 d MD (baseline 167.4 $\pm$ 14.8 vs post-3 d MD 155.6 $\pm$ 21.7 μV, $P > 0.5$, paired t test, $n = 10$; baseline HSV-G2CT vs HSV-GFP $P > 0.13$, unpaired t test; Fig. 3*D*), while once again nondeprived eye responses remained unchanged (baseline 111 $\pm$ 8 vs post-3 d MD 108 $\pm$ 9 μV, $P > 0.5$, paired t test; Fig. 3*D*).

The most parsimonious explanation for our results is that expression of G2CT in layer 4 dendrites prevents deprivation-induced depression of synapses impinging on these dendrites. It is possible, however, that the effects of HSV-G2CT infection on OD plasticity are indirect, reflecting a disruption of feedback from layer 2/3, particularly because the infections targeting layer 4 occasionally spread to layer 2/3. Arguing against this possibility is the fact that OD shifts in layer 4 can occur independently of OD shifts in layer 2/3 (14). Nonetheless, we were compelled to investigate the consequences of HSV-G2CT infections targeting layer 4 on plasticity in layer 2/3. Because the VEP method is not sensitive to changes in layer 2/3 (14), we used multichannel bundle electrode recordings of units in layer 2/3 before and after 3 days of MD in animals with HSV-G2CT infections targeted to

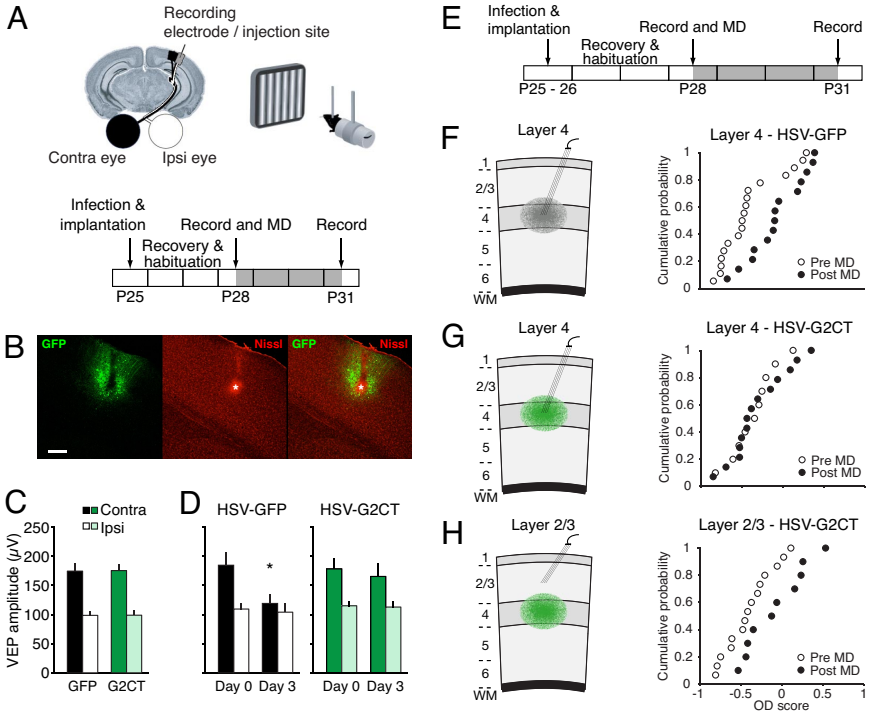

Fig. 3. Selective disruption of OD plasticity in layer 4 by HSV-G2CT. (*A*) Experimental design for monocular deprivation and VEP recordings. (*B*) Histological example verifying placement of recording electrode tip (indicated with asterisk) within the HSV infected cortical area (Scale bar, 200 μm.) (*C*) HSV-G2CT does not alter baseline VEP amplitudes. Animals were infected with HSV-GFP ($n = 14$) or HSV-G2CT ($n = 17$), and baseline VEPs were measured before random assignment into MD or SRP groups. No significant differences were observed between groups (contralateral eye response, 174.7 ± 13.5 μV vs HSV-G2CT 175.1 ± 10.9 μV, *t* test: $P > 0.9$; ipsilateral eye response, HSV-GFP 98.7 ± 8.4 μV vs HSV-G2CT 98.7 ± 7.7 μV, *t* test: $P > 0.9$). (*D*) HSV-G2CT infection blocks MD-induced synaptic depression. A significant decrease in contralateral eye VEP amplitude is observed after 3 d of MD in control (HSV-GFP) animals (baseline 184.9 ± 23.2 vs post-3 d MD 119.3 ± 15.3 μV, $P < 0.01$), whereas this decrease is blocked in animals infected with HSV-G2CT (baseline 168 ± 15 μV vs post-3 d MD 156 ± 21.7 μV, $P > 0.5$). (*E*) Experimental design for single unit recordings. (*F–H*) Infection with HSV-G2CT blocks OD plasticity in layer 4 but not layer 2/3 neurons. (*Left*) Schematics showing position of multichannel recording electrode in layer 4 (*F* and *G*) or layer 2/3 (*H*) and the targeted site of infection with HSV-GFP (*F*) or HSV-G2CT (*G* and *H*). (*Right*) Distribution of OD scores for neurons recorded either pre- or post-MD for the corresponding condition. (*F*) A significant OD shift is observed in layer 4 single units from animals infected with HSV-GFP ($n = 6$ animals, $n = 18$ neurons pre-MD, 14 post-MD, Mann–Whitney *U* test, $P = 0.01$). (*G*) The distribution of OD scores of neurons recorded from HSV-G2CT infected animals in layer 4 before and after 3 days of MD is not significantly different ($n = 3$ animals, $n = 10$ neurons pre-MD, 14 post-MD, Mann–Whitney *U* test, $P > 0.8$). (*H*) MD produces a significant shift in the distribution of OD scores of layer 2/3 neurons recorded after infection with HSV-G2CT ($n = 5$ animals, $n = 15$ neurons pre-MD, 10 post-MD, Mann–Whitney *U* test, $P < 0.05$).

layer 4. We also took this opportunity to confirm the effects of viral infection of layer 4 on OD plasticity in layer 4 by using unit recordings. The results (Fig. 3 *E–H*) clearly show an OD shift after MD in layer 2/3 but not layer 4 neurons in animals infected with HSV-G2CT. Thus, the effects of layer 4 infections with HSV-G2CT appear to be largely restricted to layer 4 neurons.

OD plasticity requires activation of NMDARs (8). Although the slice experiments revealed no defect in NMDAR-mediated synaptic transmission (Fig. 2*D*), the possibility remained that other plasticity mechanisms triggered by NMDAR activation might be nonspecifically disrupted by G2CT. Therefore, in a final series of experiments, we tested whether G2CT infection affects a newly characterized form of experience-dependent synaptic plasticity in visual cortex, termed stimulus-selective response potentiation (SRP) (15). SRP is induced by presenting awake mice with high-contrast grating stimuli of a particular orientation. Over the course of 3–4 days, the responses evoked by this grating potentiate relative to responses to gratings of other orientations. SRP requires activation of NMDARs in layer 4 of visual cortex and is believed to be mediated by delivery of AMPARs to activated thalamocortical synapses. SRP is therefore a powerful assay to determine the selectivity of G2CT effects on visual cortical plasticity.

Three groups of animals (noninfected, $n = 10$; HSV-GFP, $n = 7$; and HSV-G2CT, $n = 7$) were prepared, and VEPs elicited by monocular visual stimulation were recorded daily (Fig. S3*A*). We found that in all groups repeated presentation of grating stimuli of a single orientation resulted in a potentiation of VEPs to that stimulus during subsequent recording sessions (Fig. S3 *B–D*), approaching saturation after 3 to 4 sessions. No significant difference in SRP expression for either eye was observed between groups (repeated measures ANOVA, $P > 0.8$). These results further confirm that the blockade of OD plasticity with the G2CT peptide is unlikely to be a result of an interruption of all experience-dependent modifications.

Discussion

Although it has been shown that MD can cause internalization of postsynaptic AMPARs and LTD (4, 18), the relative contribution of this change to the OD shift was unknown. Although multiple mechanisms may participate in the modification of cortex by sensory experience (see, e.g., refs. 4, 19), the present results suggest that NMDAR-dependent AMPAR internalization is essential for the plasticity of binocular connections in layer 4.

Layer 4 receives the bulk of the geniculocortical input that brings information from the retinas into the visual cortex. The robust VEP measured in layer 4 reflects synaptic currents flowing into radially oriented dendrites in this layer, and experience-dependent changes in the VEP reflect, in large part, the modification of thalamocortical synapses (for further discussion,

see refs. 14, 15, 20). Our experimental design was influenced by 2 previous findings: (*i*) LTD in layer 4 but not layer 2/3 is blocked by intracellular loading with the G2CT peptide (4), and (*ii*) VEPs are a useful measure of plasticity in layer 4 but not layer 2/3 (14). Therefore, the contribution of LTD (AMPAR endocytosis) to OD plasticity in layer 4 was the focus of this study. We discovered, by using both VEPs and unit recordings, that the OD shift in layer 4 is prevented by expression of the G2CT peptide in layer 4 neurons. However, further research is required to see whether our conclusions generalize to synaptic plasticity in other cortical layers, particularly in light of data showing laminar diversity in the mechanisms of LTD and OD plasticity (4, 14).

The G2CT peptide was designed by Lee et al. (13) to interfere with the association of the AP2 clathrin adaptor complex with the GluR2 subunit of the AMPAR. These authors found that transfection of hippocampal neurons with the peptide blocked NMDA-stimulated AMPAR endoctyosis but had no effect on AMPA-stimulated AMPAR endocytosis. A selective effect of G2CT on NMDAR-regulated AMPAR expression was further suggested by the finding in hippocampal slices that introduction of the peptide into CA1 pyramidal neurons blocked LTD without affecting baseline synaptic transmission. Similarly, we failed to observe an increase in basal expression of AMPARs on the surface of cultured cortical neurons 24 h after infection with HSV-G2CT. Furthermore, we saw no increase in EPSCs of infected visual cortical neurons studied ex vivo, and there was no increase in the magnitude of baseline VEPs measured in vivo. Thus, our data extend the previous conclusion that constitutive endocytosis of AMPARs is not affected by the G2CT peptide. Yet, neurons expressing the peptide fail to support NMDA-stimulated AMPAR endocytosis, do not exhibit NMDAR-dependent LTD in layer 4, and importantly, do not respond to MD with a loss of visual responsiveness. We cannot rule out the possibility that chronic expression of G2CT in vivo produces an adaptive neuronal response that indirectly interferes with OD plasticity via unknown mechanism(s). However, if such an adaptive response occurs, it does not affect all forms of synaptic plasticity equally, as evidenced by the SRP experiments.

The G2CT peptide used in our study has been shown to be the minimal sequence needed to block GluR2-AP2 interaction (13). As evidenced by our experiments with the transferrin receptor, this peptide does not affect the interaction of AP-2 with all endocytic complexes. The basis for the remarkable selectivity of G2CT for NMDAR-regulated AMPAR endocytosis is currently unknown. AP-1, -2, -3, and -4 are complex heterotetramers comprised of 2 large subunits (α, γ, δ, or ε and $\beta1$, $\beta2$, $\beta3$, or $\beta4$) and 2 small subunits ($\mu1$–4 and $\sigma1$–4) (21). These subunits contain binding sites for specific adaptors and specific cargoes, as well as clathrin. The affinity of each AP-2 molecule for a target thus varies based on its subunit composition. It is therefore possible that G2CT specifically blocks the binding of GluR2 with AP-2 without affecting other AP-2 binding events. Indeed, a peptide inhibitor of GluR4/AP-2 interaction has been shown to be insufficient in blocking GluR2/AP-2 interaction in vitro (13). Whatever the explanation, our experiments show empirically that G2CT has no observable effect on the fairly extensive range of neuronal properties we examined both in vitro and in vivo, with the exception of NMDAR-dependent synaptic depression.

The current findings bridge multiple levels of analysis to establish that one molecular mechanism for LTD is functionally significant in the brain. Although it has been known for almost 2 decades that NMDARs are critical for visual cortical plasticity (8, 22), their precise contribution had not been pinpointed. The G2CT peptide is far more selective than NMDAR blockade or genetic deletion, but the effect on OD plasticity is just as robust. Thus, our findings provide strong support for the "LTD hypothesis" of visual cortical plasticity that weak activation of NMDARs by poorly correlated inputs from the deprived eye is a key trigger for the loss of visual responsiveness after MD (2).

Materials and Methods

Subjects. Male C57BL/6 mice were used for all experiments. Animals were group-housed and kept on a 12-h light/dark cycle. All animals were treated in accordance with National Institutes of Health and Massachusetts Institute of Technology guidelines.

HSV Vector Construction. HSV-GFP was generated by using the unaltered p1005+ HSV-amplicon bicistronic plasmid containing a complete CMV-GFP expression cassette as the second cistron. HSV-G2CT was generated by inserting a 50-bp fragment encoding the G2CT peptide (KRMKLNINPS) (13) into the first cistron downstream of the HSV IE 4/5 promoter. Additional details available in Fig. S1.

Biochemical Measurement of Surface Receptors. For assays with dissociated neurons, cortical cultures (14–18 DIV) were prepared and infected with HSV vectors (1–2 multiplicity of infection, MOI) 20–24 h before biotinylation experiments. Cultures were rinsed with warm DMEM and treated with NMDA (20 μM, 3 min). After brief rinses, conditioned medium was added back and plates were incubated at 37 °C for 30 min. Surface receptors were biotinylated with 1.5 mg/mL Sulfo-NHS-SS-biotin (Pierce) for 20 min on ice. Cultures were rinsed and solubilized with RIPA buffer. Soluble extracts containing equal amounts of protein were incubated with Immobilized Neutravidin agarose (80 μL; Pierce) overnight at 4 °C, washed, then resuspended in SDS sample buffer (40 μL) and boiled. Quantitative immunoblotting was performed on biotinylated surface proteins by using antibodies to TfR (Chemicon) and to Glur1 (Upstate). An antibody to GluR1 was used due to the limited amounts of sample necessitating stripping and reprobing after visualization of TfR protein levels. It should be noted that previous research has shown that activity-dependent changes in GluR2/3 and GluR1 subunit levels within the visual cortex mirror one another and are highly correlated (18).

TfR internalization assays were performed as described in ref. 23 with minor changes. Briefly, after preincubation with leupeptin (100 μg/mL, 30 min), cultures were with 1 mg/mL Sulfo-NHS-SS-biotin in D-PBS on ice (20 min). Whereas control samples remained on ice, experimental samples were treated with 40 μg/mL transferrin in D-PBS (30 min, 37 °C). Biotinylated receptors remaining or recycled back to the surface were stripped with glutathione buffer for 15 min (2×) and quenched with iodoacetamide (5 mg/mL, 3 × 5 min). Cells were lysed with RIPA buffer, and biotinylated proteins were purified as described in *Materials and Methods*. To control for nonspecific binding and entrance of biotin into cells, data from transferrin-treated samples were normalized to control samples maintained at 4 °C.

For biochemical assays using cortical slices, viral vectors were unilaterally injected into visual cortex 2 days before biochemical assay. For all HSV infections, a small volume of virus (1–1.5 μL total) was injected into the binocular visual cortex 450 μm below dural surface at a rate of 0.1 μL/min. Visual cortical slices were prepared from both hemispheres 2 days post infection as described in ref. 18. After recovery (1–2 h) in ACSF, slices were transferred to a NMDA (100 μM) containing chamber and incubated (15 min). Slices were transferred back to a recovery chamber and incubated for 20 min. HSV-infected and corresponding control areas from the opposing hemisphere were microdissected, homogenized in RIPA buffer, and processed as described above by using antibodies to the GluR1 and GluR2/3 subunits of AMPARs (Upstate). Additional methods are available as *SI Text*.

In Vitro Slice Electrophysiology. Mice were injected in the visual cortex unilaterally with HSV-G2CT as described above, and acute slices were prepared 48–72 h later as described in ref. 4. Layer 4 pyramidal neurons exhibiting GFP fluorescence and neurons from the control noninfected hemisphere were patched under IR-DIC. Experiments showing a >20% change in R_s were excluded, as were cells with a resting membrane potential less negative than −50 mV. When possible, attempts were made to record from control and G2CT-expressing neurons in slices prepared from the same animal on the same day. Baseline EPSCs were evoked (0.05 Hz) under voltage clamp (−65 mV) with a bipolar stimulating electrode (FHC) placed in the white matter. Following a stable baseline, input-output curves were recorded, and a stimulation intensity yielding a half-maximal response was chosen for further study. For LTD experiments, a stable baseline was recorded for 10 min, and LTD was induced by pairing 600 pulses at 1 Hz with depolarization of the postsynaptic neuron to −40 mV (4).

AMPA/NMDA ratios were determined essentially as described in ref. 24 by using holding potentials of −90 and +40 mV. At each holding potential, 4–6 responses were recorded at 0.05 Hz; responses showing polysynaptic activity

were excluded from analysis. The ratio of AMPA to NMDA amplitude was calculated for HSV-G2CT infected neurons and normalized to the ratio obtained in control neurons. After recording, slices were stained for biocytin to confirm that all included neurons were spiny and located in layer 4. Additional methods are available as *SI Text*.

In Vivo Electrophysiology. Electrode implantation, monocular deprivation, and SRP induction were performed as described (15, 17). Briefly, VEPs were measured in binocular visual cortex (3 mm lateral of lambda), by using tungsten microelectrodes (FHC) inserted 450 μm below the cortical surface. VEPs were elicited in awake, head-restrained mice by using full-field, sine-wave gratings (0.05 cyc/deg, 100% contrast) with a fixed temporal frequency (1Hz). For SRP experiments, 200–400 stimuli were randomly presented daily to each eye (15). Animals were injected with HSV-GFP or HSV-G2CT as described in *Materials and Methods* and subsequently implanted with a recording electrode at the site of injection. At the end of experimentation, animals were euthanized and brains removed for histological analysis.

Single unit recordings were performed by using chronically implanted multichannel bundle electrodes implanted into layer 2/3 or 4 immediately after viral infusion targeted to layer 4. Spiking activity was evoked in awake mice as above and recorded by using commercially available hardware and software. Output from each recording electrode was split, directed to preamplifiers, band-passed filtered for spikes (300–3,000 Hz) and for local field potentials (1–300 Hz), and sent to a PC running the data acquisition software. For recorded spikes, offline discrimination of single unit activity was based on waveform shape, whereas multiunit activity was excluded. Spike trains were smoothed by convolution with a Gaussian kernel, and spontaneous activity (recorded during viewing of a blank screen) was subtracted. The maximum response to stimulation of each eye (IE, ipsilateral eye; CE, contralateral eye) above spontaneous firing rate was used to calculate the OD score, defined as (IE - CE)/(IE + CE) (14, 25).

ACKNOWLEDGMENTS. We thank Robert Crozier, Mikhail Frenkel, Jason Coleman, Asha Bhakar, Emily Osterweil, Erik Sklar, and Suzanne Meagher for assistance. This work was partly supported by grants from the National Institutes of Health.

1. Bear MF (2003) Bidirectional synaptic plasticity: From theory to reality. *Philos Trans R Soc Lond B Biol Sci* 358:649–655.
2. Bear MF, Cooper LN, Ebner FF (1987) A physiological basis for a theory of synapse modification. *Science* 237:42–48.
3. Malenka RC, Bear MF (2004) LTP and LTD: An embarrassment of riches. *Neuron* 44:5–21.
4. Crozier RA, Wang Y, Liu CH, Bear MF (2007) Deprivation-induced synaptic depression by distinct mechanisms in different layers of mouse visual cortex. *Proc Natl Acad Sci USA* 104:1383–1388.
5. Feldman DE, Nicoll RA, Malenka RC, Isaac JT (1998) Long-term depression at thalamocortical synapses in developing rat somatosensory cortex. *Neuron* 21:347–357.
6. Kirkwood A, Bear MF (1994) Homosynaptic long-term depression in the visual cortex. *J Neurosci* 14:3404–3412.
7. Markram H, Lubke J, Frotscher M, Sakmann B (1997) Regulation of synaptic efficacy by coincidence of postsynaptic APs and EPSPs. *Science* 275:213–215.
8. Bear MF, Kleinschmidt A, Gu Q, Singer W (1990) Disruption of experience-dependent synaptic modifications in striate cortex by infusion of an NMDA receptor antagonist. *J Neurosci* 10:909–925.
9. Daw NW, et al. (1999) Injection of MK-801 affects ocular dominance shifts more than visual activity. *J Neurophysiol* 81:204–215.
10. Roberts EB, Meredith MA, Ramoa AS (1998) Suppression of NMDA receptor function using antisense DNA block ocular dominance plasticity while preserving visual responses. *J Neurophysiol* 80:1021–1032.
11. Rao Y, Daw NW (2004) Layer variations of long-term depression in rat visual cortex. *J Neurophysiol* 92:2652–2658.
12. Malinow R, Malenka RC (2002) AMPA receptor trafficking and synaptic plasticity. *Annu Rev Neurosci* 25:103–126.
13. Lee SH, Liu L, Wang YT, Sheng M (2002) Clathrin adaptor AP2 and NSF interact with overlapping sites of GluR2 and play distinct roles in AMPA receptor trafficking and hippocampal LTD. *Neuron* 36:661–674.
14. Liu CH, Heynen AJ, Shuler MG, Bear MF (2008) Cannabinoid receptor blockade reveals parallel plasticity mechanisms in different layers of mouse visual cortex. *Neuron* 58:340–345.
15. Frenkel MY, et al. (2006) Instructive effect of visual experience in mouse visual cortex. *Neuron* 51:339–349.
16. Neve RL, Neve KA, Nestler EJ, Carlezon WA, Jr (2005) Use of herpes virus amplicon vectors to study brain disorders. *Biotechniques* 39:381–391.
17. Frenkel MY, Bear MF (2004) How monocular deprivation shifts ocular dominance in visual cortex of young mice. *Neuron* 44:917–923.
18. Heynen AJ, et al. (2003) Molecular mechanism for loss of visual cortical responsiveness following brief monocular deprivation. *Nat Neurosci* 6:854–862.
19. Maffei A, Nataraj K, Nelson SB, Turrigiano GG (2006) Potentiation of cortical inhibition by visual deprivation. *Nature* 443:81–84.
20. Sawtell NB, et al. (2003) NMDA receptor-dependent ocular dominance plasticity in adult visual cortex. *Neuron* 38:977–985.
21. Knuehl C, et al. (2006) Novel binding sites on clathrin and adaptors regulate distinct aspects of coat assembly. *Traffic* 7:1688–1700.
22. Bear MF, Coleman H (1990) Binocular competition in the control of geniculate cell size depends opon visual cortical *N*-methyl-D-aspartate receptor activation. *Proc Natl Acad Sci USA* 87:9246–9249.
23. Ehlers MD (2000) Reinsertion or degradation of AMPA receptors determined by activity-dependent endocytic sorting. *Neuron* 28:511–525.
24. Myme CI, Sugino K, Turrigiano GG, Nelson SB (2003) The NMDA-to-AMPA ratio at synapses onto layer 2/3 pyramidal neurons is conserved across prefrontal and visual cortices. *J Neurophysiol* 90:771–779.
25. Rittenhouse CD, Shouval HZ, Paradiso MA, Bear MF (1999) Monocular deprivation induces homosynaptic long-term depression in visual cortex. *Nature* 397: 347–350.